Particlelike Phonon Propagation Dominates Ultralow Lattice Thermal Conductivity in Crystalline Tl_{3}VSe_{4}

Yi Xia, Koushik Pal, Jiangang He, Vidvuds Ozoliņš, and Chris Wolverton

Phys. Rev. Lett. **124**, 065901 — Published 14 February 2020

DOI: 10.1103/PhysRevLett.124.065901

Particle-Like Phonon Propagation Dominates Ultralow Lattice Thermal Conductivity in Crystalline Tl_3VSe_4

Yi Xia,[1,*] Koushik Pal,[1] Jiangang He,[1] Vidvuds Ozoliņš,[2,3] and Chris Wolverton[1,†]

[1] *Department of Materials Science and Engineering, Northwestern University, Evanston, IL 60208, USA*
[2] *Department of Applied Physics, Yale University, New Haven, CT 06511, USA*
[3] *Energy Sciences Institute, Yale University, West Haven, CT 06516, USA*

(Dated: January 23, 2020)

We investigate the microscopic mechanisms of ultralow lattice thermal conductivity (κ_l) in Tl_3VSe_4 by combining a first-principles density-functional theory (DFT) based framework of anharmonic lattice dynamics with the Peierls-Boltzmann transport equation (PBTE) for phonons. We include contributions of the three- and four-phonon scattering processes to the phonon lifetimes as well as the temperature-dependent anharmonic renormalization of phonon energies arising from an unusually strong quartic anharmonicity in Tl_3VSe_4. In contrast to a recent report by Mukhopadhyay *et al.* [Science 360, 1455 (2018)] which suggested that a significant contribution to κ_l arises from random walks among uncorrelated oscillators, we show that particle-like propagation of phonon excitations can successfully explain the experimentally observed ultralow κ_l. Our findings are further supported by explicit calculations of the off-diagonal terms of the heat-current operator, which are found to be small and indicate that wave-like tunneling of heat-carrying vibrations is of minor importance. Our results (i) resolve the discrepancy between the theoretical and experimental κ_l, (ii) offer new insights into the minimum κ_l achievable in Tl_3VSe_4, and (iii) highlight the importance of high-order anharmonicity in low-κ_l systems. The methodology demonstrated here may be used to resolve the discrepancies between the experimentally measured and the theoretically calculated κ_l in skutterides and perovskites, as well as to understand the glasslike κ_l in complex crystals with strong anharmonicity, leading towards the goal of rational design of new materials.

Understanding of thermal transport in crystalline compounds with ultralow lattice thermal conductivity κ_l is fundamentally interesting because such materials bridge the gap between the particle-like propagation of phonon wavepackets in typical crystals and the off-diagonal coupling and diffusion of localized vibrational modes in disordered systems such as glasses [1]. Materials with ultralow values of κ_l also have useful technological applications as thermoelectrics, thermal barrier coatings, and in data storage devices [2–5]. Despite significant effort [6–9], comprehensive understanding of the heat transport in crystals with κ_l near the amorphous limit remains an outstanding challenge [10] because the phonon mean free path (MFP) approaches the interatomic separation and the conventional description based on propagating lattice phonons starts to break down. A successful empirical model was introduced by G. Slack [11], which has guided design and experimental demonstration of ultralow κ_l in crystalline compounds with large unit cells and complex structures, such as clathrates [12, 13] and skutterudites [14, 15]. In contrast, ultralow κ_l is relatively rare in simple crystals with small unit cells.

Recently, Mukhopadhyay *et al.* [16] experimentally reported an ultralow value of $\kappa_l = 0.30 \pm 0.05$ W/(m·K) [17] at $T = 300$ K in crystalline Tl_3VSe_4. This is highly unusual considering that Tl_3VSe_4 has a simple body-centered cubic lattice (space group $I\bar{4}3m$) with only eight atoms in its primitive cell, as shown in Fig. 1(d). To explain the observed value of κ_l, Mukhopadhyay *et al.* proposed a complex scenario of heat transport that involves two channels: lattice phonons and localized oscillators. Their proposal was largely based on the results of calculations using the Peierls-Boltzmann Transport Equation (PBTE) [18] with 3rd-order anharmonicity in the conventional phonon picture. These calculations resulted in a value of $\kappa_l = 0.16$ W/(m·K) at $T = 300$ K, which is only approximately half of the experimental value [0.30 ± 0.05 W/(m·K)]. It was noted that the MFPs of many phonons were predicted to fall below the interatomic separation due to low group velocities and strong anharmonicity, possibly invalidating the foundational assumptions of PBTE. To resolve the discrepancy between the theoretical and experimental κ_l in Tl_3VSe_4, the authors proposed a phenomenological two-channel model, which consists of two separate vibrational transport channels, namely, (i) propagating particle-like phonon wave packets and (ii) random walk (hopping) among uncorrelated localized oscillators [16]. The resulting κ_l shows a significantly improved agreement with the experiments in both magnitude and temperature dependence, suggesting that the hopping channel contributes as much as the conventional transport by phonon wave packets. However, the observed Raman spectra, specific heat, and temperature-dependence of $\kappa_l(T)$ only revealed features characteristic of phonons in an ordered crystalline compound. Since the interpretation given by Mukhopadhyay *et al.* [16] relies heavily on the calculated phononic contributions to κ_l within the lowest order of

* yimaverickxia@gmail.com
† c-wolverton@northwestern.edu

the perturbation theory (PT), it is important to ascertain that this picture still holds when higher-order anharmonic interactions and temperature-dependent phonon frequency shifts are included. The possibility of strong high-order anharmonicity has already been indicated by the large discrepancy between the theoretical and experimental mean square displacements of Tl atoms in Ref. [16]. It is thus important to understand the physics of heat transport in Tl_3VSe_4 when lattice dynamical effects beyond the third-order anharmonicity are included.

Here, we perform first-principles calculations based on the density-functional theory (DFT) to study the physics of κ_l in Tl_3VSe_4 by explicitly including effects arising from quartic anharmonicity. We show that this treatment leads to a giant finite-temperature renormalization of the low-lying phonon modes. The calculated phonon scattering rates for the processes involving these renormalized phonons are significantly reduced in comparison with the values obtained without renormalization. The overall effect of the quartic anharmonicity, including both three- and four-phonon processes, increases the calculated κ_l to a value that is in good agreement with experiments. Our results show that particle-like phonon propagation can by itself explain the measured ultralow κ_l in Tl_3VSe_4, without invoking the second transport channel via uncorrelated oscillators.

We first discuss the current state-of-the-art in anharmonic lattice dynamics (ALD) and place our work within the hierarchy of increasingly accurate methods. In the phonon quasiparticle picture, κ_l is usually modeled by combining a microscopic potential energy model with ALD perturbation series [20, 21] and PBTE [18, 22], the latter of which can be solved in various flavors [23–27]. Particularly, solving the linearized PBTE under the single mode approximation leads to a simple expression for thermal conductivity, $\kappa_l = \frac{1}{NV}\sum_\lambda C_\lambda \mathbf{v}_\lambda \otimes \mathbf{v}_\lambda \tau_\lambda$, where N, V, C_λ, $\mathbf{v}_\lambda$ and τ_λ are the number of sampled phonon wave vectors, volume of the primitive cell, phonon mode heat capacity, group velocity, and lifetime, respectively (λ is a composite index for the wave vector and dispersion branch). In practice, κ_l is always calculated under some approximations. The lowest level of theory uses a harmonic (HA) description of the phonon energy ω_λ and an anharmonic estimation of the lifetime τ_λ considering only three-phonon (3ph) interactions due to cubic anharmonicity [26, 28–38]. Within this theory, Mukhopadhyay *et al.* [16] showed that the calculated κ_l of Tl_3VSe_4 is seriously underestimated, which served as a motivation for their two-channel model. However, this level of theory often fails to accurately predict κ_l in compounds with strong high-order anharmonicity, which among other consequences may lead to substantial anharmonic phonon frequency renormalization at finite temperatures due to phonon-phonon interactions [20, 39–44]. This has motivated theoretical developments and computational implementations to explicitly treat such higher-order terms. To account for the anharmonic renormalization arising from high-order (or particularly quartic) anharmonicity, the self-consistent phonon (SCPH) approximation [45–48] has been recently integrated with first-principles calculations to gain a better estimation of ω_λ by several authors [49–57]. In a related development, a formula to explicitly evaluate the phonon scattering rates ($1/\tau_\lambda$) due to the four-phonon (4ph) interactions has been derived by Feng and Ruan [58]. Applying this to the theoretically predicted ultra-high κ_l compound BAs [59], Feng, Lindsay and Ruan have shown that the 4ph scattering is comparable in strength with the 3ph scattering [60], resulting in a much reduced κ_l; this has been confirmed both experimentally and theoretically [61–63]. Most recently, it has been demonstrated by Xia [64] and Ravichandran *et al.* [65] that to correctly reproduce the magnitude and temperature dependence of

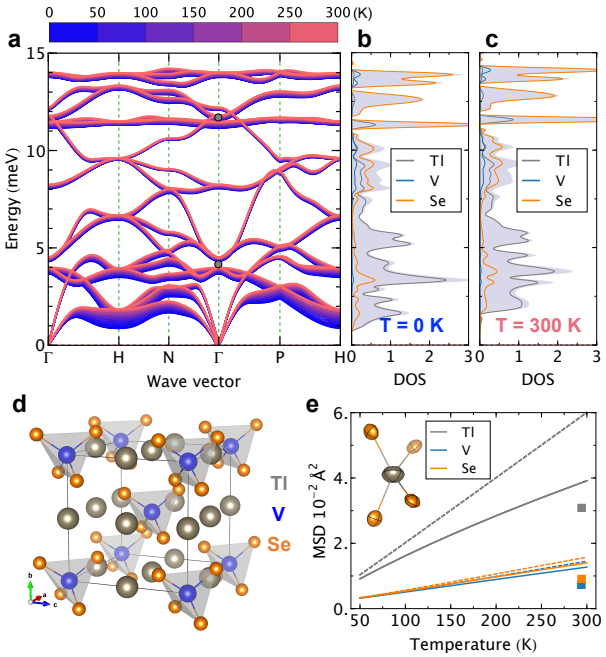

FIG. 1. (a) Calculated temperature-dependent phonon dispersions from $T = 0$ K to 300 K. The disks at the Γ point depict the experimental measurements at 300 K [16]. (b) and (c) Atom-decomposed phonon density of states (DOS) at $T = 0$ K and 300 K, respectively. The shaded gray areas depict the total DOS. (d) Crystal structure of Tl_3VSe_4, which features a sublattice formed by VSe_4^{3-} tetrahedral units with loosely bound Tl atoms, visualized using VESTA software [19]. (e) Comparison of theoretical (solid/dashed lines) and experimental (squares) temperature-dependent atomic mean square displacements (MSD) along the [111] direction for Tl (gray), V (blue) and Se (orange) atoms. The dashed lines are calculated in the harmonic (HA) approximation, and the solid lines are from the self-consistent phonon (SCPH) approximation. The inset depicts the anisotropic thermal displacement ellipsoids of Tl and Se atoms with the principal ellipses denoted by black solid lines.

experimental κ_l in strongly anharmonic compounds such as PbTe and NaCl, one needs to take into account quartic anharmonicity for both ω_λ and τ_λ. These schemes can be thought of as a ladder of approximations based on the level of theory for modeling ω_λ and τ_λ, as shown in Fig. 2(a). In this study, we utilized a level of theory with the highest accuracy available today within the framework of ALD and PBTE under the single mode relaxation time approximation, namely, SCPH+3,4ph, where ω_λ is anharmonically renormalized at finite temperatures based on the SCPH approximation and τ_λ is calculated with both 3ph and 4ph scattering processes among the renormalized phonons, as well as the isotope scattering and extrinsic scattering due to the grain boundaries (see details below) [22, 66–68]. We refer the readers to the Supplemental Material (SM) [69] for more details of our approach [70].

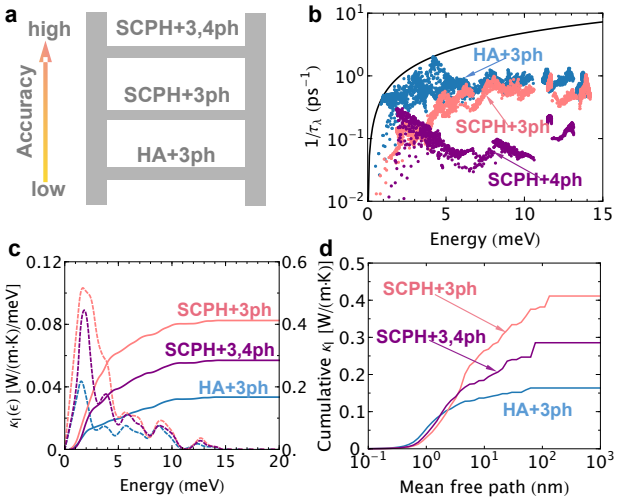

FIG. 2. (a) A schematic showing the ladder of approximations for calculating κ_l. The levels of theory with accuracy from low to high are: HA+3ph, SCPH+3ph and SCPH+3,4ph, where HA and SCPH denote respectively the harmonic (without renormalization) and self-consistent phonon approximations (with renormalization) for calculating phonon energy, and 3/4ph denote three/four-phonon scattering processes considered in computing phonon scattering rates. (b) Comparison of 3ph scattering rates ($1/\tau_\lambda$) calculated in the HA (blue) and the SCPH (pink) approximations, respectively. The purple dots depict the calculated 4ph scattering rates in the SCPH approximation. The solid black line assumes the scattering rate to be twice the vibrational frequency, as adopted in the Cahill model [7] to estimate minimum κ_l. (c) Comparison of cumulative (solids lines) and differential (dashed lines) κ_l calculated using different levels of theory. (d) Same as (c) but for the mean free path cumulative κ_l. All results were obtained at $T = 300$ K.

We begin by examining the impact of quartic anharmonicity on ω_λ. Fig. 1(a) shows the calculated phonon dispersion from $T = 0$ to 300 K, which reveals a significant hardening of the low-lying modes below 5 meV with increasing temperature. These modes are dominated by the vibrations of Tl atoms, as revealed by the atom-decomposed phonon density of states in Figs. 1(b) and (c). In contrast, the high-lying optical modes corresponding to the majority Se and V vibrations are only slightly hardened. This interesting vibrational feature associated with the Tl atoms resembles the behavior of rattling phonon modes in the so-called cage compounds, whose energies display small values but exhibit strong temperature dependence [56, 71]. The analogy is made stronger by the loose bonding strength of Tl atoms [16] and by the experimentally observed anomalously large mean-square displacements (MSD) at 300 K [16]. Physically, the hardening of the low-lying phonon modes stems from a U-shaped potential energy surface with a strongly positive quartic coefficient (an example of the lowest-lying phonon mode at the H point is given in Fig.S3 in SM [69]).

The observed strong anharmonic phonon hardening further manifests in the improved agreement between the calculated MSDs and experimental data. We see in Fig. 1(e) that the calculated MSD of Tl atoms in the harmonic approximation is 0.060 Å^2 at $T = 300$ K, which compares well to the slightly larger value of 0.067 Å^2 calculated in Ref.[16], but is nearly twice as large as the experimentally measured value of 0.031 Å^2. In striking contrast, the SCPH approximation significantly reduces the discrepancy, giving rise to a value of 0.039 Å^2 [72]. This improved agreement between theory and experiment shows that the hardened Tl vibrations suppress the phonon population and thereby decrease the MSD, revealing the essential role of quartic anharmonicity. Note that additional frequency shift could also arise from cubic anharmonicity [20, 40, 73–75], which is not considered here but might be used to further resolve the slightly overestimated MSD from theory. It is worth mentioning that a large discrepancy in heat capacity between theory and experiment has been reported at low temperatures ($T < 10$ K) in Tl_3VSe_4 [16]. Since the renormalization is weak at low temperatures, we find that this discrepancy persists in our SCPH calculations (see Fig.S4(a) in SM [69]), suggesting that it could be caused by lattice imperfections inherent in the synthesized samples.

With an improved description of the phonon quasiparticle energy at hand, we move on to investigate κ_l by exploring how the quartic anharmonicity affects the key ingredients entering PBTE, namely, ω_λ, $\mathbf{v}_\lambda$, and the scattering rate ($1/\tau_\lambda$). We find that replacing the ω_λ and $\mathbf{v}_\lambda$ in the HA+3ph calculations with the renormalized ones leads to negligible increment in κ_l from 0.16 W/(m·K) to 0.17 W/(m·K) at 300 K. This indicates that τ_λ plays a more dominant role than ω_λ and $\mathbf{v}_\lambda$ in altering κ_l. Indeed, as shown in Fig. 2(b), 3ph scattering rates are significantly reduced when phonons are anharmonically hardened, which can be ultimately traced back to the suppressed three-phonon scattering

phase space [56, 64, 71]. This leads to a remarkable increase in κ_l from 0.16 W/(m·K) to 0.41 W/(m·K) at 300 K when the lowest level of theory (HA+3ph) is improved by considering anharmonic renormalization (SCPH+3ph). Meanwhile, the 4ph scattering rates are roughly as high as those of the 3ph processes, particularly for the phonon modes with energies around 2 meV. As a result, SCPH+3,4ph leads to a reduced κ_l of 0.29 W/(m·K), which is in excellent agreement with the experimental value of 0.30 ± 0.05 W/(m·K).

We conclude that the highest ladder of theory can fully explain the heat transfer in Tl_3VSe_4 in terms of the particle-like phonon wave packet propagation picture without using adjustable parameters and without invoking *ad hoc* assumptions about a secondary transport channel. The validity of the phonon picture, qualitatively different from the two-channel model proposed by Mukhopadhyay *et al.* [16], is largely restored by including the effects of quartic anharmonicity. As discussed by Allen and Feldman [8], in order for the PBTE approach to work well, each phonon mode should have either (i) an MFP long enough to define its wave vector or (ii) a lifetime (τ_λ) long enough to define its frequency. It is evident from our results that the overall scattering rates ($1/\tau_\lambda$) are significantly reduced [see Fig. 2(b)] and MFPs (see Fig.S4 (c) in SM [69]) are enhanced in comparison with the HA+3ph theory level, thus making the phonon picture relevant again [76]. We note that these renormalized phonons for which the particle-like propagation applies are not harmonic but are quasiparticle excitations corresponding to the poles of the Greens function [77], which preserve a well-defined relation between the frequency and the wave vector and can form propagating wave packets.

The energy-cumulative and differential κ_l in Fig. 2(c) show that the major contributions to the enhanced κ_l computed with SCPH+3,4ph relative to HA+3ph are from the phonon modes with energies below 5 meV, consistent with their significantly reduced scattering rates. The MFP-cumulative κ_l in Fig. 2(d) indicates that heat carrying phonons have fairly large MFPs with a maximum value of about 100 nm at $T = 300$ K. The phonon picture of thermal transport implies that an even lower κ_l may be achieved through nanostructuring (e.g., less than 0.20 W/(m·K) if the maximum MFP is limited to 10 nm).

We compare the temperature-dependent κ_l calculated using three different levels of theory in Fig. 3(a). The overall effect of the quartic anharmonicity on κ_l in the whole temperature range qualitatively resembles those at $T = 300$ K. Quantitative analysis shows that higher temperature tends to increase the relative enhancement in κ_l. Specifically, comparing the results obtained from HA+3ph and SCPH+3,4ph, the relative enhancement in κ_l sees an increase, percentage-wise, from 14% at $T = 50$ K to 70% at 300 K. However, even though the enhancement of κ_l is relatively small at low temperatures, it leads to a nonnegligible overestimation compared to the experimental data below 200 K. We attribute this disagreement to extrinsic phonon scattering processes due to the grain boundaries and lattice imperfections, which are not included in the SCPH+3,4ph model. We show in Fig. 3(b) the effect of grain boundary scattering on κ_l as functions of grain size. It can be seen that κ_l is significantly modified in both the magnitude and temperature dependence, particularly at low temperatures. This, of course, is consistent with the weakened multiphonon interactions and enhanced intrinsic MFPs at low T. It is worth noting that using an average grain size of about 0.2 μm, which is used to match measured κ_l at 6 K[16], leads to a $\kappa_l \propto T^{-0.64}$ that nicely agrees with experimentally observed $T^{-0.65}$, as well as magnitude.

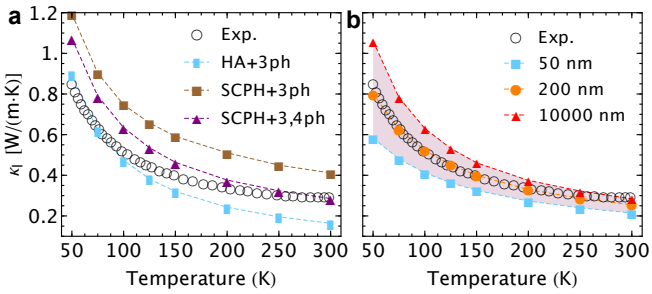

FIG. 3. (a) Temperature-dependent κ_l calculated at three levels of theory in comparison with experimental measurements [16]. (b) Calculated κ_l (shaped region) considering additional phonon-grain boundary scattering on top of SCPH+3,4ph. Grain sizes ranging from 50 nm to 10000 nm are considered.

The above calculated κ_l using the PBTE approach, despite achieving remarkable agreement with the experiments, only includes the diagonal terms of the heat current operator [8, 78]. A comprehensive treatment of the heat current operators requires additional off-diagonal terms which correspond to the heat conduction related to the wave-like tunneling and the loss of coherence between different vibrational eigenstates [79]. Recently, a unified theory of thermal transport in crystals and disordered solids has been independently developed by Simoncelli *et al.* [79] and Isaeva *et al.* [80], making it possible to explicitly evaluate the off-diagonal terms. Our estimation of the off-diagonal contributions on top of the SCPH+3,4ph results gives an increment of 0.08 W/(m·K) to κ_l at 300 K, leading to a total κ_l of 0.34 W/(m·K) when the additional grain boundary (0.2 μm) scattering is considered, which is still within the experimental value of 0.30 ± 0.05 W/(m·K) at 300 K. Although such an increment may not be negligible as a result of the intrinsically very low κ_l, it is still significantly smaller than the heat conduction from the particle-like phonon propagation. It is worth noting that a much earlier attempt by

Srivastava has identified negligibly small contribution to κ_l from the off-diagonal terms in covalently bonded germanium crystal [81]. Additionally, the second heat conduction channel in the proposed two-channel model [16], which is based on the Cahill-Watson-Pohl model [7, 82] and adopts a wave-length dependent mean free path [83], is fundamentally different from the off-diagonal terms of the heat current operator.

In summary, we have used a state-of-the-art first-principles scheme, which is capable of explicitly treating the effects of quartic anharmonicity on both phonon quasiparticle energies and lifetimes, to investigate the lattice thermal transport in crystalline Tl_3VSe_4. Our results show that the lattice thermal conductivity of crystalline Tl_3VSe_4 can be explained by the heat transfer due to the particle-like phonon propagation, with only a small portion from non-diagonal contributions due to the wave-like tunneling between different phonon states. Our study unveils that a comprehensive understanding of the physical mechanisms underlying ultralow lattice thermal conductivity in crystalline compounds can be achieved by employing highly accurate theoretical treatment that goes beyond the phenomenological model. Our model that further includes off-diagonal contributions to κ_l might be used to explore the physical mechanisms underlying the glasslike κ_l in complex crystalline compounds with intrinsic strong anharmonicity.

Y.X. acknowledges support from Toyota Research Institute (TRI) through the Accelerated Materials Design and Discovery program (methodology development). Y.X., K.P., J.H. and C.W. acknowledge support from the U.S. Department of Energy, Office of Science and Office of Basic Energy Sciences, under Award No. DE-SC0014520 (DFT calculations). V.O. acknowledges financial support from the National Science Foundation Grant DMR-1611507. This research used resources of the National Energy Research Scientific Computing Center, a DOE Office of Science User Facility supported by the Office of Science of the U.S. Department of Energy under Contract No. DE-AC02-05CH11231. Y.X. thanks Michele Simoncelli for useful discussions.

[1] D. G. Cahill and R. O. Pohl, Annual Review of Physical Chemistry **39**, 93 (1988).
[2] L. E. Bell, Science **321**, 1457 (2008).
[3] J. Sootsman, D. Chung, and M. Kanatzidis, Angewandte Chemie International Edition **48**, 8616 (2009).
[4] D. Rowe, *CRC Handbook of Thermoelectrics* (CRC-Press, 1995).
[5] G. Nolas, J. Sharp, and J. Goldsmid, *Thermoelectrics: Basic Principles and New Materials Developments*, Springer Series in Materials Science (Springer Berlin Heidelberg, 2001).
[6] A. Einstein, Annalen der Physik **340**, 679 (1911).
[7] D. G. Cahill, S. K. Watson, and R. O. Pohl, Phys. Rev. B **46**, 6131 (1992).
[8] P. B. Allen and J. L. Feldman, Phys. Rev. B **48**, 12581 (1993).
[9] W. Lv and A. Henry, Scientific Reports **6**, 35720 EP (2016).
[10] J. J. Freeman and A. C. Anderson, Phys. Rev. B **34**, 5684 (1986).
[11] G. A. Slack (Academic Press, 1979) pp. 1 – 71.
[12] G. S. Nolas, J. L. Cohn, G. A. Slack, and S. B. Schujman, Applied Physics Letters **73**, 178 (1998).
[13] J. L. Cohn, G. S. Nolas, V. Fessatidis, T. H. Metcalf, and G. A. Slack, Phys. Rev. Lett. **82**, 779 (1999).
[14] D. T. Morelli and G. P. Meisner, Journal of Applied Physics **77**, 3777 (1995).
[15] B. C. Sales, D. Mandrus, and R. K. Williams, Science **272**, 1325 (1996).
[16] S. Mukhopadhyay, D. S. Parker, B. C. Sales, A. A. Puretzky, M. A. McGuire, and L. Lindsay, Science **360**, 1455 (2018).
[17] This uncertainty mostly comes from the accuracy of determining the dimensions of the sample, as stated in the Supplementary Materials of Ref. [16].
[18] R. Peierls, *Quantum Theory of Solids*, International Series of Monographs on Physics (Clarendon Press, 1996).
[19] K. Momma and F. Izumi, Journal of Applied Crystallography **41**, 653 (2008).
[20] A. A. Maradudin and A. E. Fein, Phys. Rev. **128**, 2589 (1962).
[21] A. A. Maradudin, A. E. Fein, and G. H. Vineyard, physica status solidi (b) **2**, 1479 (1962).
[22] J. Ziman, *Electrons and Phonons: The Theory of Transport Phenomena in Solids*, International series of monographs on physics (OUP Oxford, 1960).
[23] M. Omini and A. Sparavigna, Physica B: Condensed Matter **212**, 101 (1995).
[24] M. Omini and A. Sparavigna, Phys. Rev. B **53**, 9064 (1996).
[25] L. Chaput, Phys. Rev. Lett. **110**, 265506 (2013).
[26] G. Fugallo, M. Lazzeri, L. Paulatto, and F. Mauri, Phys. Rev. B **88**, 045430 (2013).
[27] A. Cepellotti and N. Marzari, Phys. Rev. X **6**, 041013 (2016).
[28] A. Debernardi, S. Baroni, and E. Molinari, Phys. Rev. Lett. **75**, 1819 (1995).
[29] A. J. H. McGaughey and M. Kaviany, Phys. Rev. B **69**, 094303 (2004).
[30] D. A. Broido, M. Malorny, G. Birner, N. Mingo, and D. A. Stewart, Appl. Phys. Lett. **91**, 231922 (2007).
[31] J. E. Turney, E. S. Landry, A. J. H. McGaughey, and C. H. Amon, Phys. Rev. B **79**, 064301 (2009).
[32] J. Garg, N. Bonini, B. Kozinsky, and N. Marzari, Phys. Rev. Lett. **106**, 045901 (2011).
[33] K. Esfarjani, G. Chen, and H. T. Stokes, Phys. Rev. B **84**, 085204 (2011).
[34] L. Chaput, A. Togo, I. Tanaka, and G. Hug, Phys. Rev. B **84**, 094302 (2011).
[35] W. Li, J. Carrete, N. A. Katcho, and N. Mingo, Computer Physics Communications **185**, 1747 (2014).
[36] A. Togo, L. Chaput, and I. Tanaka, Phys. Rev. B **91**, 094306 (2015).
[37] L. Lindsay, C. Hua, X. Ruan, and S. Lee, Materials Today Physics **7**, 106 (2018).
[38] A. J. H. McGaughey, A. Jain, H.-Y. Kim, and B. Fu, Journal of Applied Physics **125**, 011101 (2019).

[39] P. Choquard, *The Anharmonic Crystal*, Frontiers in Physics (Benjamin, 1967).
[40] R. A. Cowley, Reports on Progress in Physics **31**, 123 (1968).
[41] H. R. Clyde and M. L. Klein, C R C Critical Reviews in Solid State Sciences **2**, 181 (1971).
[42] T. Barron, M. Klein, and N. R. C. O. C. O. (Ont.), *Perturbation Theory of Anharmonic Crystals* (Defense Technical Information Center, 1974).
[43] G. Srivastava, *The Physics of Phonons* (Taylor & Francis, 1990).
[44] D. Wallace, *Thermodynamics of Crystals*, Dover books on physics (Dover Publications, 1998).
[45] D. Hooton, The London, Edinburgh, and Dublin Philosophical Magazine and Journal of Science **46**, 422 (1955).
[46] T. R. Koehler, Phys. Rev. Lett. **17**, 89 (1966).
[47] N. R. Werthamer, Phys. Rev. B **1**, 572 (1970).
[48] M. L. Klein and G. K. Horton, Journal of Low Temperature Physics **9**, 151 (1972).
[49] P. Souvatzis, O. Eriksson, M. I. Katsnelson, and S. P. Rudin, Phys. Rev. Lett. **100**, 095901 (2008).
[50] I. Errea, B. Rousseau, and A. Bergara, Phys. Rev. Lett. **106**, 165501 (2011).
[51] O. Hellman, I. A. Abrikosov, and S. I. Simak, Phys. Rev. B **84**, 180301 (2011).
[52] I. Errea, M. Calandra, and F. Mauri, Phys. Rev. B **89**, 064302 (2014).
[53] T. Tadano and S. Tsuneyuki, Phys. Rev. B **92**, 054301 (2015).
[54] A. van Roekeghem, J. Carrete, and N. Mingo, Phys. Rev. B **94**, 020303 (2016).
[55] G. A. S. Ribeiro, L. Paulatto, R. Bianco, I. Errea, F. Mauri, and M. Calandra, Phys. Rev. B **97**, 014306 (2018).
[56] Y. Xia and V. Ozoliņš, arXiv e-prints , arXiv:1903.08800 (2019), arXiv:1903.08800 [cond-mat.mtrl-sci].
[57] U. Aseginolaza, R. Bianco, L. Monacelli, L. Paulatto, M. Calandra, F. Mauri, A. Bergara, and I. Errea, Phys. Rev. Lett. **122**, 075901 (2019).
[58] T. Feng and X. Ruan, Phys. Rev. B **93**, 045202 (2016).
[59] L. Lindsay, D. A. Broido, and T. L. Reinecke, Phys. Rev. Lett. **111**, 025901 (2013).
[60] T. Feng, L. Lindsay, and X. Ruan, Phys. Rev. B **96**, 161201 (2017).
[61] J. S. Kang, M. Li, H. Wu, H. Nguyen, and Y. Hu, Science **361**, 575 (2018).
[62] S. Li, Q. Zheng, Y. Lv, X. Liu, X. Wang, P. Y. Huang, D. G. Cahill, and B. Lv, Science **361**, 579 (2018).
[63] F. Tian, B. Song, X. Chen, N. K. Ravichandran, Y. Lv, K. Chen, S. Sullivan, J. Kim, Y. Zhou, T.-H. Liu, M. Goni, Z. Ding, J. Sun, G. A. G. Udalamatta Gamage, H. Sun, H. Ziyaee, S. Huyan, L. Deng, J. Zhou, A. J. Schmidt, S. Chen, C.-W. Chu, P. Y. Huang, D. Broido, L. Shi, G. Chen, and Z. Ren, Science **361**, 582 (2018).
[64] Y. Xia, Applied Physics Letters **113**, 073901 (2018).
[65] N. K. Ravichandran and D. Broido, Phys. Rev. B **98**, 085205 (2018).
[66] S.-i. Tamura, Phys. Rev. B **27**, 858 (1983).
[67] S.-i. Tamura, Phys. Rev. B **30**, 849 (1984).
[68] H. Casimir, Physica **5**, 495 (1938).
[69] "Supplementary materials contain details on the theory, computational parameters, and convergence tests.".
[70] DFT [84] calculations were performed using the Vienna *Ab Initio* Simulation Package (VASP) [85–88]. The projector-augmented wave (PAW) [89] method was used in conjunction with the Perdew-Burke-Ernzerhof revised PBEsol [90, 91] version of the generalized gradient approximation (GGA) [92] for the exchange-correlation functional [84]. Harmonic interatomic force constants (IFCs) were extracted using the finite-displacement approach implemented in Phonopy [93], and anharmonic IFCs up to quartic terms were extracted using compressive sensing lattice dynamics (CSLD) [94]. Numerical calculations of ALD and PBTE were performed using the ShengBTE package [35, 95] with an in-house implementation of the SCPH+3,4ph scheme (see SM [69], which includes additional Refs. [96–100]).
[71] T. Tadano and S. Tsuneyuki, Phys. Rev. Lett. **120**, 105901 (2018).
[72] We have found that this observation persists no matter whether PBE or PBEsol functional is used, indicating that it is independent of the details of the DFT calculations.
[73] E. R. Cowley, Journal of Physics C: Solid State Physics **5**, 1345 (1972).
[74] R. D. Valle, P. Fracassi, R. Righini, and S. Califano, Chemical Physics **74**, 179 (1983).
[75] S. Narasimhan and D. Vanderbilt, Phys. Rev. B **43**, 4541 (1991).
[76] Another criterion can be resorted to the Ioffe-Regel limit [101], wherein the most relevant quantity should be the magnitude of the periodicity vector instead of interatomic distance. Considering the small unit cell of the material under consideration, it is still not critical enough to invalidate the phonon particle picture.
[77] G. Mahan, *Many-Particle Physics*, Physics of Solids and Liquids (Springer, 2000).
[78] R. J. Hardy, Phys. Rev. **132**, 168 (1963).
[79] M. Simoncelli, N. Marzari, and F. Mauri, Nature Physics (2019), 10.1038/s41567-019-0520-x.
[80] L. Isaeva, G. Barbalinardo, D. Donadio, and S. Baroni, Nature Communications **10**, 3853 (2019).
[81] G. Srivastava, Le Journal de Physique Colloques **42**, C6 (1981).
[82] D. G. Cahill and R. Pohl, Solid State Communications **70**, 927 (1989).
[83] M. T. Agne, R. Hanus, and G. J. Snyder, Energy Environ. Sci. **11**, 609 (2018).
[84] P. Hohenberg and W. Kohn, Phys. Rev. **136**, B864 (1964).
[85] G. Kresse and J. Hafner, Phys. Rev. B **47**, 558 (1993).
[86] G. Kresse and J. Hafner, Phys. Rev. B **49**, 14251 (1994).
[87] G. Kresse and J. Furthmüller, Comput. Mater. Sci. **6**, 15 (1996).
[88] G. Kresse and J. Furthmüller, Phys. Rev. B **54**, 11169 (1996).
[89] P. E. Blöchl, Phys. Rev. B **50**, 17953 (1994).
[90] J. P. Perdew, K. Burke, and M. Ernzerhof, Phys. Rev. Lett. **77**, 3865 (1996).
[91] J. P. Perdew, A. Ruzsinszky, G. I. Csonka, O. A. Vydrov, G. E. Scuseria, L. A. Constantin, X. Zhou, and K. Burke, Phys. Rev. Lett. **100**, 136406 (2008).
[92] J. P. Perdew, K. Burke, and Y. Wang, Phys. Rev. B **54**, 16533 (1996).
[93] A. Togo and I. Tanaka, Scripta Materialia **108**, 1 (2015).
[94] F. Zhou, W. Nielson, Y. Xia, and V. Ozoliņš, Phys.

Rev. Lett. **113**, 185501 (2014).
[95] W. Li, L. Lindsay, D. A. Broido, D. A. Stewart, and N. Mingo, Phys. Rev. B **86**, 174307 (2012).
[96] T. Feng, X. Yang, and X. Ruan, Journal of Applied Physics **124**, 145101 (2018).
[97] Y. Wang, J. J. Wang, W. Y. Wang, Z. G. Mei, S. L. Shang, L. Q. Chen, and Z. K. Liu, Journal of Physics: Condensed Matter **22**, 202201 (2010).
[98] S. Baroni and R. Resta, Phys. Rev. B **33**, 7017 (1986).
[99] M. Gajdoš, K. Hummer, G. Kresse, J. Furthmüller, and F. Bechstedt, Phys. Rev. B **73**, 045112 (2006).
[100] E. Candès and M. Wakin, IEEE Signal Proc. Mag. **25**, 21 (2008).
[101] A. F. Ioffe and A. R. Regel, "Progress in semiconductors," (John Wiley & Sons, Inc., New York, 1960) p. 239.